Article

Discovery Medicine 2024; 36(184): 1070–1079
https://doi.org/10.24976/Discov.Med.202436184.99

Astragaloside IV Mediates the PI3K/Akt/mTOR Pathway to Alleviate Injury and Modulate the Composition of Intestinal Flora in ApoE$^{-/-}$ Atherosclerosis Model Rats

Dongwen Sun[1], Yiqiang Wang[2], Bingyao Pang[3], Lihong Jiang[2,*]

[1]College of Traditional Chinese Medicine, Changchun University of Chinese Medicine, 130117 Changchun, Jilin, China
[2]Department of Cardiology, The Affiliated Hospital of Changchun University of Chinese Medicine, 130021 Changchun, Jilin, China
[3]Department of Liver, Spleen and Stomach Diseases, The Affiliated Hospital of Changchun University of Chinese Medicine, 130021 Changchun, Jilin, China
*Correspondence: mango612118@163.com (Lihong Jiang)
Published: 20 May 2024

Background: Atherosclerosis (AS) is a chronic inflammatory vascular disease with a complex pathogenesis. Astragaloside IV (AST IV), the primary active component of Astragalus, possesses anti-inflammatory, antioxidant, and immunomodulatory properties. This research aims to investigate the outcome of AST IV on AS and its potential molecular mechanism.
Methods: A high-fat diet (21% fat, 50% carbohydrate, 20% protein, 0.15% cholesterol, and 34% sucrose) was utilized to feed Apolipoprotein E deficient (ApoE$^{-/-}$) SD rats for 8 weeks, followed by continuous intragastric administration of AST IV for 8 weeks. Biochemical detection was conducted for serum lipid levels and changes in vasoactive substances. After Masson staining, aortic root oil red O staining, and Hematoxylin Eosin (HE) staining, the efficacy of AST IV was verified using quantitative reverse transcription polymerase chain reaction (qRT-PCR). The mRNA expression levels of inflammatory factors and endothelial dysfunction-related biomarkers in rat aortic root tissues were appraised. The changes in the composition of intestinal flora in rats after AST IV treatment were appraised using Image J (Multi-point Tool). Western blot was used to evaluate phosphatidylinositol-3-kinase/protein kinase B/mammalian target of rapamycin (PI3K/Akt/mTOR) pathway-related protein levels in rat aortic root tissues.
Results: AST IV administration alleviated the pathological symptoms of AS rats. AST IV administration reduced serum total cholesterol (TC), triglycerides (TG), low-density lipoprotein cholesterol (LDL-C), endothelin-1 (ET-1) and angiotensin (Ang)-II (Ang-II) levels, and augmented serum high-density lipoprotein cholesterol (HDL-C) and nitric oxide (NO) levels. At the same time, AST IV administration inhibited the levels of tumor necrosis factor-α (TNF-α), interleukin-6 (IL-6), IL-1β, vascular cell adhesion molecule-1 (VCAM-1), matrix metalloproteinase-2 (MMP-2), macrophage inflammatory protein-1 (MCP-1), and intercellular adhesion molecule-1 (ICAM-1) in the aortic root tissue of AS rats. In addition, the intestinal flora changed significantly after AST IV administration. The number of Bifidobacterium, Lactobacillus, and Bacteroides augmented significantly, and *Enterobacter*, *Enterococcus*, *Fusobacterium*, and *Clostridium* significantly decreased. Mechanistically, AST IV administration inhibited the phosphorylation of PI3K, Akt, and mTOR in AS rats. When combined with Dactolisib (BEZ235) (a PI3K/Akt/mTOR pathway inhibitor), AST IV could further inhibit phosphorylation and reduce inflammation.
Conclusion: AST IV has a potential anti-AS effect, which can improve the pathological changes of the aorta in ApoE$^{-/-}$ rats fed with a high-fat diet, reduce the level of inflammatory factors, and modulate the composition of intestinal flora via the PI3K/Akt/mTOR pathway.

Keywords: astragaloside IV; atherosclerosis; gut microbiota; PI3K/Akt/mTOR

Introduction

Atherosclerosis (AS) is a chronic inflammatory vascular disease and the pathological basis for the occurrence and development of most cardiovascular diseases, seriously endangering human health [1]. The pathogenesis of AS is complex and related to the increase of low-density lipoprotein cholesterol (LDL-C), vascular endothelial dysfunction, inflammation, and oxidative stress [2–4]. At present, the combination of antiplatelet and cholesterol-lowering drugs (mainly aspirin combined with statins) is the mainstream method for the treatment of AS. However, the role of these drugs in AS is limited, and the significant risk of developing cardiovascular disease still exists [5,6]. Therefore, more effective treatment strategies and means are urgently needed.

In recent years, multiple studies have confirmed that intestinal flora change is closely related to the occurrence and development of AS disease [7,8]. The intestinal flora is considered a complex ecosystem in the gastrointestinal environment, composed of bacteria, archaea, fungi, viruses, and protozoa, gut microbiota can affect lipid metabolism and lipid levels in the blood and tissues of rats and humans [9]. Dyslipidemia-related diseases, such as non-alcoholic liver disease and AS, are associated with changes in gut microbiota [10]. Zhang *et al*. [11] have shown that Dingxin Recipe IV could increase the relative abundance of *Muribaculaceae* and *Ruminococcaceae*, reduce the abundance of *Erysipelotrichaceae*, and improve atherosclerosis in Apolipoprotein E deficient ($ApoE^{-/-}$) rats fed with a high-fat diet by regulating intestinal flora. Research has shown that *Bifidobacterium* and *Lactobacillus* can play an anti-AS role by improving blood lipids and reducing oxidative stress and inflammation [12].

Astragaloside IV (AST IV) is the main active ingredient of Astragalus membranaceous, which has many biological functions such as anti-inflammatory, anti-oxidation, immune regulation, and anti-tumor; AST IV can prevent a variety of diseases, including cardiovascular disease, nervous system disease, lung disease, diabetes, organ damage, kidney disease and gynecological diseases [13]. AST IV relieves atherosclerosis in Low Density Lipoprotein Receptor (LDLR) ($^{-/-}$) rats [14]. The outcome and potential mechanism of AST IV on $ApoE^{-/-}$ rats fed with a high-fat diet were appraised in this research.

Materials and Methods

Experimental Animals

Twenty-four male SPF-grade $ApoE^{-/-}$ SD rats and 6 wild-type control SD rats weighing 200 ± 20 g, aged 6–7 weeks (Sibeifu Biotechnology Co., Ltd., SCXK (Beijing) 2021–0006, Beijing, China). The animals were employed separately in SPF standard cages, with an ambient temperature, a light/dark cycle of 12 h, a standard diet and free drinking water, and adaptive feeding for 1 week.

Experimental Grouping and Processing

The rats were divided into 5 subgroups (n = 6): (1) normal control subgroup (CON) was wild-type SD rats with a normal diet for 16 weeks. (2) The Western diet, which contains 21% fat, 50% carbohydrate, 20% protein, 0.15% cholesterol, and 34% sucrose, was employed to feed $ApoE^{-/-}$ SD rats in the Model subgroup (Beijing Huafukang Biotechnology Co., Ltd., H10141, Beijing, China) for 8 weeks. (3) AST IV subgroup was $ApoE^{-/-}$ SD rats. After 8 weeks of Western diet feeding, 20 mg/(kg·d) AST IV (purity ≥90%, Merck, PHL89377, Shanghai, China) was intragastrically administered for 8 weeks [15]. (4) Simvastatin subgroup: $ApoE^{-/-}$ SD rats were fed with the Western diet for 8 weeks and then given 5 mg/(kg·d) Simvastatin by gavage for 8 weeks (Sigma-Aldrich, S6196, Shanghai, China) [16]. (5) The AST IV + Dactolisib (BEZ235) subgroup was $ApoE^{-/-}$ SD rats. After 8 weeks of Western diet feeding, 20 mg/(kg·d) AST IV and 2.5 mg/d BEZ235 were intragastrically administered for 8 weeks (MCE, HY-50673, Shanghai, China) [17]. The body weight of rats was measured weekly, and the daily food intake was recorded. After the administration, fresh rat feces were collected, anesthetized rats (2% pentobarbital sodium (30mg/kg)) were subjected to abdominal aortic blood collection, and serum was collected after centrifugation for testing. Rats were anesthetized with 2% pentobarbital sodium (30mg/kg) and sacrificed by cervical dislocation. Aortic root tissue was collected for subsequent experiments.

Detection of Serum Biochemical Index

Total cholesterol (TC, E-BC-K109-M), triglycerides (TG, E-BC-K261-M), LDL-C (E-BC-K205-M), high-density lipoprotein cholesterol (HDL-C, E-BC-K221-M), nitric oxide (NO, E-BC-K035-M), endothelin-1 (ET-1, E-EL-R1458) and angiotensin (Ang)-II (E-EL-R1430) levels in serum were appraised according to the kit instructions. All kits were obtained from Elabscience Biotechnology Co., Ltd. (Wuhan, China).

Oil Red O Staining

4% paraformaldehyde was employed to fix collected aortic root tissue (Beyotime, P0099, Shanghai, China). Conventional paraffin-embedded sections were immersed in oil red O solution (Abcam, ab223796, Shanghai, China) for 10 min. Subsequently, the sections were placed in 75% alcohol until the staining site was bright red, then stained with hematoxylin (Servicebio, G1040, Wuhan, China), differentiated back to blue, and mounted. For each section, three fields of view were randomly chosen and photographed under a microscope (DM1000, Leica, Wetzlar, Germany). Quantitative analysis was conducted employing Image J software (National Institutes of Health, version 1.4, Bethesda, MD, USA).

Masson Staining

According to the kit's instructions, an experimental operation was conducted (Solarbio, G1340, Beijing, China). After the frozen sections were thawed and fixed, the sections were immersed in Masson A1 solution and Masson A2 solution mixed in equal proportion, Masson B solution, Masson C solution, Masson D solution, Masson E solution, Masson F solution, Masson G staining solution, rinsed, differentiated and dehydrated, and then sealed. For each section, three fields of view were randomly chosen and photographed under a microscope (Leica, DMi8, Wetzlar, Germany). Quantitative analysis was conducted employing Image J software (ImageJ2, NIH, Bethesda, MD, USA).

Table 1. Primer sequence for qRT-PCR.

Gene name	Primer	Sequence (5′–3′)
Tumor necrosis factor-α (*TNF-α*)	Forward	AGGCGCTCCCCAAGAAGACA
	Reverse	TCCTTGGCAAAACTGCACCT
Interleukin-6 (*IL-6*)	Forward	GCCTTCGGTCCAGTTGCCTT
	Reverse	GCAGAATGAGATGAGTTGTC
IL-1β	Forward	GCAGTCTACACAGCTTCGGG
	Reverse	CCGCCTCAGCCTCCCAAAG
Vascular cell adhesion molecule-1 (*VCAM-1*)	Forward	CCCTTGACCGGCTGGAGATT
	Reverse	TGGGGGCAACATTGACATAAAGTG
Matrix metalloproteinase-2 (*MMP-2*)	Forward	AGACAAAGAGTTGGCAGTGCAAT
	Reverse	CTGTATGTGATCTGGTTCTTGTCCC
Macrophage inflammatory protein-1 (*MCP-1*)	Forward	CCCCAGTCACCTGCTGTTAT
	Reverse	CCACAATGGTCTTGAAGATCAC
Intercellular adhesion molecule-1 (*ICAM-1*)	Forward	CAGTGACCATCTACAGCTTTCCGG
	Reverse	GCTGCTACCACAGTGATGACAA
GAPDH	Forward	GGGAAACTGTGGCGTGAT
	Reverse	GAGTGGGTGTCGCTGTTGA

qRT-PCR, quantitative reverse transcription polymerase chain reaction.

Hematoxylin Eosin (HE) Staining

After thawing and fixing, the frozen sections were stained with hematoxylin (Servicebio, G1004, Wuhan, China), differentiated with 1% hydrochloric acid ethanol, stained with eosin (Solarbio, E8090, Beijing, China), dehydrated, and sealed using transparent and neutral resin. For each section, 3 fields of view were randomly chosen and photographed under a microscope (Leica, DMi8, Weitzlar, Germany).

Quantitative Reverse Transcription Polymerase Chain Reaction (qRT-PCR)

Employing Trizol (Ambion, 15596026, Carlsbad, CA, USA), total RNA was extracted from aortic root tissue. According to the instructions of PrimeScript RT Reagent Kit (Takara, RR037A, Dalian, China), RNA was reversely transcribed into cDNA and employed as a template. The reaction system was established according to the instructions of the SYBR FAST qPCR Master Mix kit (KAPA Biosystems, KM4101, Boston, MA, USA) for fluorescence quantitative PCR detection. The reaction tube was placed in the MX3000P Realtime PCR reactor (Agilent Technologies Inc., New York, CA, USA). Reaction procedure: 95 °C 3 min; 95 °C 5 s, 56 °C 10 s, 72 °C 25 s, a total of 40 cycles. The Ct value was obtained after the reaction, *GAPDH* was employed as the internal reference, and the $2^{-\Delta\Delta Ct}$ method was employed for statistical analysis. Primer sequences are shown in Table 1, synthesized by Wuhan Saiweier Biotechnology Co., Ltd. (China).

Determination of the Number of Intestinal Flora

The collected rat feces were placed in a volumetric flask containing glass beads and sterile water. The microbial particles were shaken in a shaker at 120 r/min for 30 min to disperse the microbial particles fully. The suspension was diluted to 10^6 by 10 times gradient dilution. A total of 100 µL dilutions were inoculated into TPY agar medium (Solarbio, LA5590, Beijing, China), MRS agar medium (Solarbio, M8330, Beijing, China), *Enterococcus* agar medium (Solarbio, LA4070, Beijing, China), violet red bile glucose agar medium (Solarbio, LA2360, Beijing, China), *Fusobacterium* selective agar medium (Solarbio, LA4720, Beijing, China), enhanced *Clostridium* agar medium (Solarbio, LA4370, Beijing, China) and BDS medium (Solarbio, LA7030, Beijing, China). *Bifidobacterium*, *Lactobacillus*, *Enterobacter*, *Enterococcus*, *Fusobacterium*, *Clostridium*, and *Bacteroides* were cultured in an anaerobic environment (nitrogen:hydrogen:oxygen = 80:10:10) at 37 °C for 48 h, and the colonies were counted.

Western Blot

Total protein was extracted from aortic root tissue using a radioimmunoprecipitation assay lysis buffer (Beyotime, 87788, Shanghai, China). A bicinchoninic acid kit (Beyotime, 786-570, Beijing, China) was employed for quantification. 20 µg of protein was isolated by 10% sodium dodecyl sulfate-polyacrylamide gel electrophoresis (SDS-page) and transferred to polyvinylidene fluoride membranes (Millipore, IPVH00010, Billerica, MA, USA). 5% skimmed milk powder (Solarbio, D8340, Beijing, China) was sealed overnight at 4 °C. Primary antibodies: phospho-phosphatidylinositol-3-kinase (p-PI3K, 1:1000, Abcam, ab182651, Shanghai, China), phosphatidylinositol-3-kinase (PI3K, 1:1000, Bioswamp, PAB42067, Wuhan, China), phospho-protein kinase B (p-Akt, 1:1000, Abcam, ab38449, Shanghai, China), protein kinase B (Akt, 1:1000, Bioswamp, Wuhan, China), phospho-mammalian target

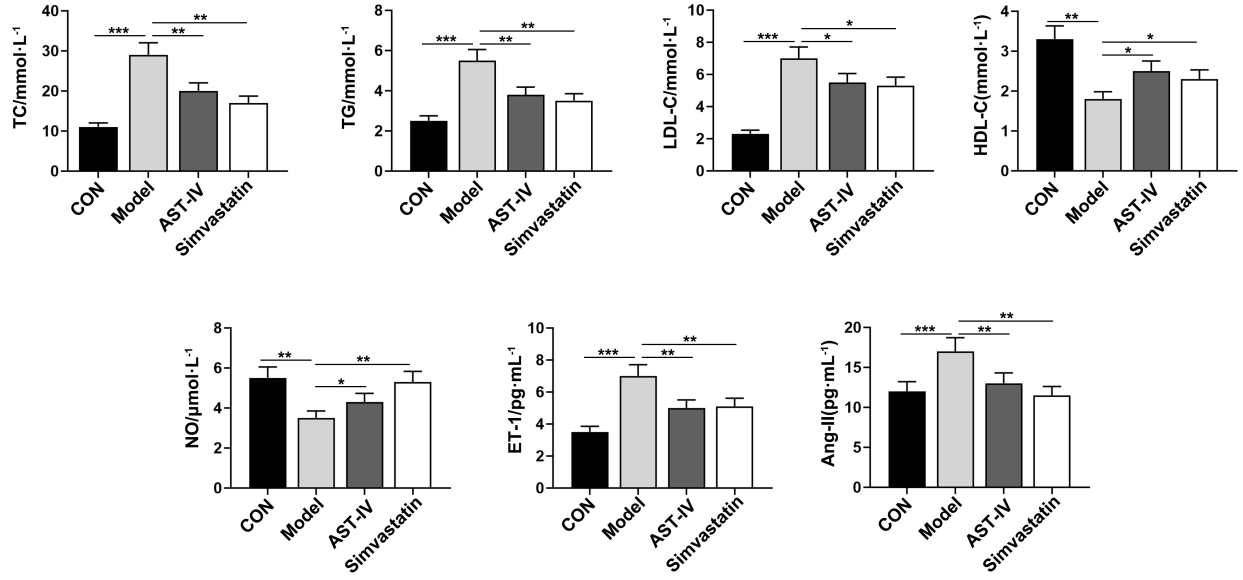

Fig. 1. AST IV improved blood lipid levels in AS rats. TC, TG, LDL-C and HDL-C, NO, ET-1, and Ang-II levels in serum were appraised. n = 6. *$p < 0.05$, **$p < 0.01$, ***$p < 0.001$. CON, normal control subgroup; AST IV, astragaloside IV; AS, atherosclerosis; TC, total cholesterol; TG, triglycerides; LDL-C, low-density lipoprotein cholesterol; HDL-C, high-density lipoprotein cholesterol; NO, nitric oxide; ET-1, endothelin-1; Ang-II, angiotensin-II.

of rapamycin (p-mTOR, 1:1000, Proteintech, 67778-1-Ig, Wuhan, China), mammalian target of rapamycin (mTOR, 1:1000, Proteintech, 66888-1-Ig, Wuhan, China), GAPDH (1:1000, ABclonal, AC004, Wuhan, China) were added and incubated for 12 h. The cells were incubated with goat anti-rabbit IgG secondary antibody (1:2000, Solarbio, K1034G-AF594, Beijing, China) for 1 h. ECL chemiluminescence Kit (Thermo Fisher Scientific, WP20005, Shanghai, China) was employed for exposure development. Bio-Tanon imaging system (Tanon Science & Technology Co., Ltd., Shanghai, China) was used for visualization, imaging, and quantification, and GAPDH was employed as an endogenous control. Image J software (ImageJ2, NIH, Bethesda, MA, USA) was employed to analyze each protein band's gray value and calculate the target protein's relative expression.

Statistical Analysis

The SPSS 22.0 software (IBM, Armonk, NY, USA) was employed for statistical analysis. All data were presented as the mean and standard deviation (mean ± SD). The difference between the two subgroups was analyzed by Student's *t*-tests. Differences among subgroups were compared by one-way ANOVA, followed by a post-hoc test (Tukey's method). $p < 0.05$ represents a significant difference.

Results

AST IV Improved Blood Lipid Levels in AS Rats

For exploring the outcome of AST IV on blood lipids in AS rats, serum TC, TG, LDL-C, and HDL-C levels were appraised. TC, TG, and LDL-C levels in the serum of the Model subgroup were substantially augmented, and the level of HDL-C was eased significantly in contrast with the CON subgroup. Versus the Model subgroup, TC, TG, and LDL-C levels in the serum of the AST IV and Simvastatin subgroups were eased significantly, and the level of HDL-C was augmented significantly. Next, the effect of AST IV on vasoactive substances in AS rats was explored. Compared to the CON subgroup, the NO level in the Model subgroup was eased significantly, and the levels of ET-1 and Ang-II were augmented significantly. In contrast with the Model subgroup, the levels of NO in the serum of the AST IV subgroup and Simvastatin subgroup were augmented significantly, and the levels of ET-1 and Ang-II were eased significantly. These results indicate that AST IV can improve the blood lipid level of AS rats and modulate the dynamic balance of active substances released by vascular endothelial cells (Fig. 1).

AST IV Alleviated Aortic Root Pathological Damage and Inflammatory Response in AS Rats

Oil red O staining confirmed the absence of lipid accumulation in the CON subgroup. In contrast, the Model subgroup exhibited a significant increase in lipid accumulation within the aortic root, as evidenced by a marked increase in the percentage of oil red O staining. The lipid accumulation in the aortic root of the AST IV and Simvastatin subgroups was eased, and the oil red O staining percentage was eased substantially compared to the Model subgroup (Fig. 2A,B). Masson staining validated no fibrosis in the aortic root of the CON subgroup. In contrast with

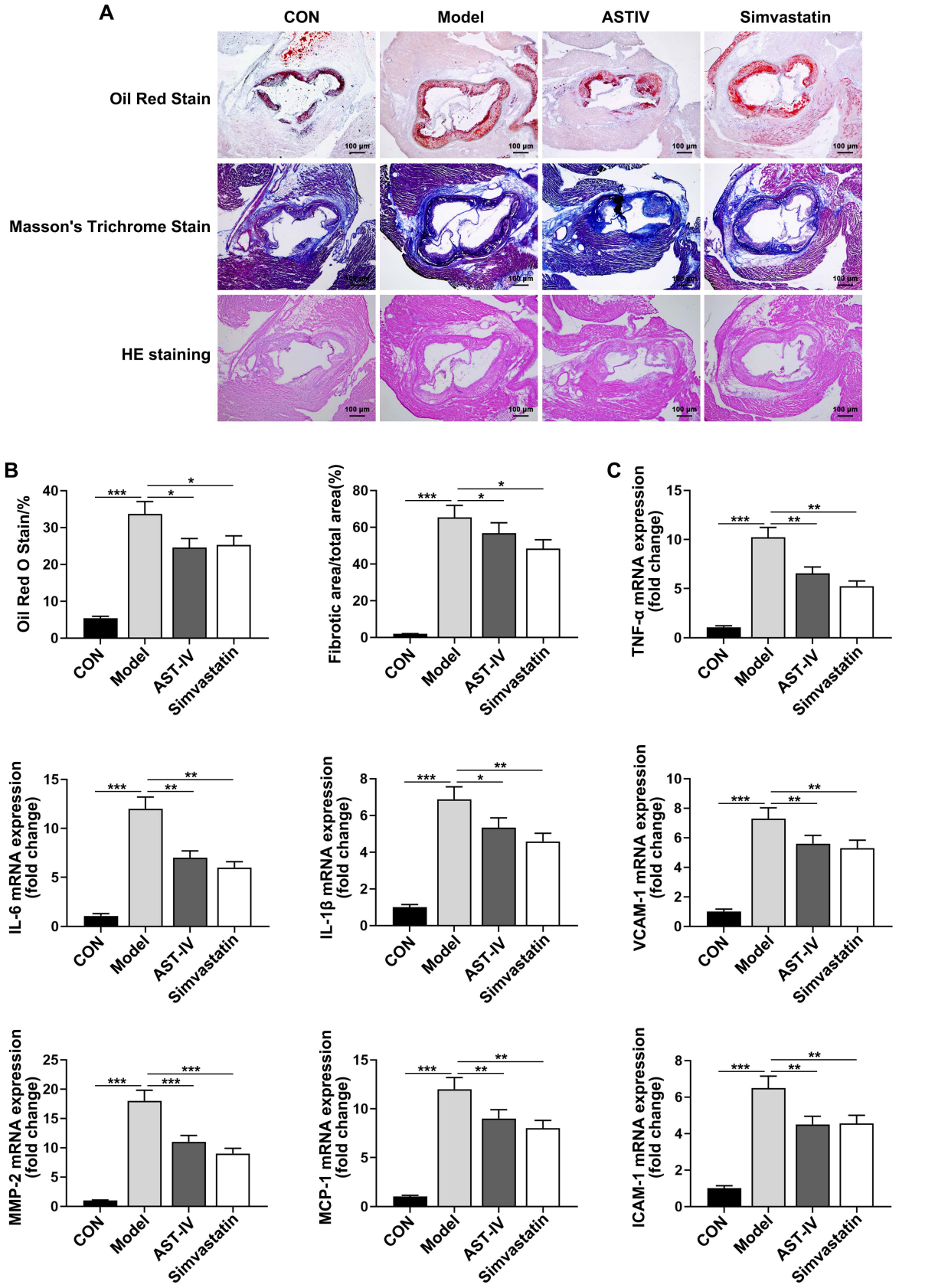

Fig. 2. AST IV alleviated aortic root pathological damage and inflammatory response in AS rats. (A) Oil red O staining, Masson staining, and HE staining of rat aortic root tissue. (B) Quantitative analysis of oil red O staining and Masson staining. (C) In rat aortic root tissues, via qRT-PCR, *TNF-α*, *IL-6*, *IL-1β*, *VCAM-1*, *MMP-2*, and *ICAM-1* mRNA were appraised. n = 6. *$p < 0.05$, **$p < 0.01$, ***$p < 0.001$. HE, Hematoxylin Eosin.

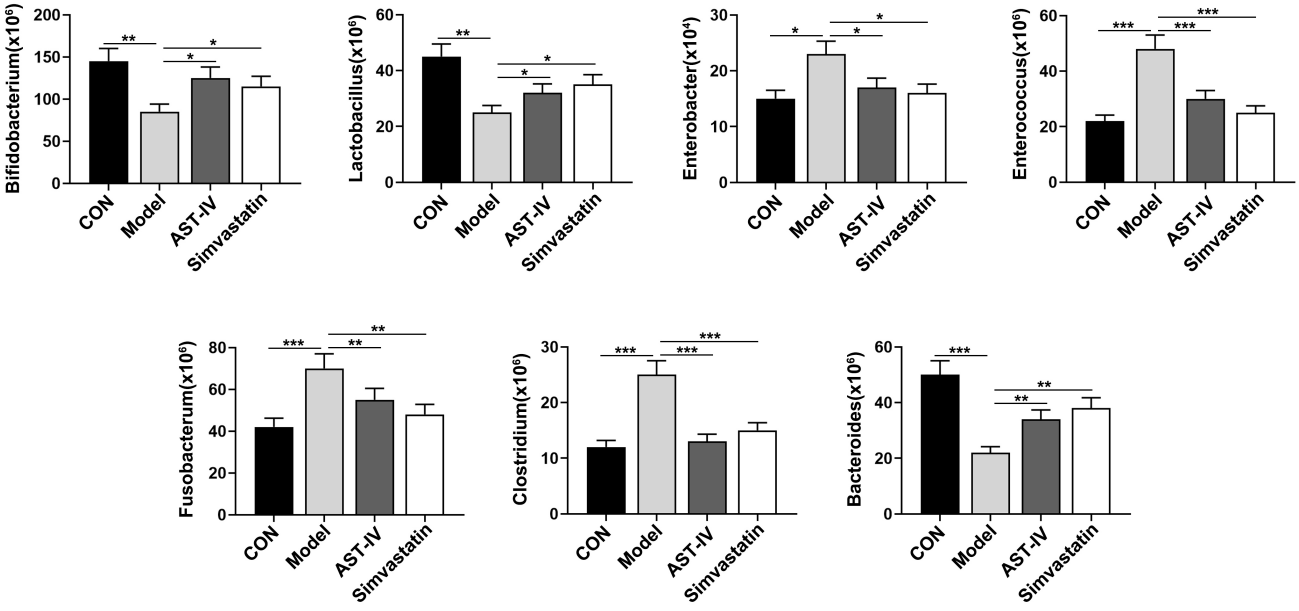

Fig. 3. AST IV could modulate the composition of intestinal flora in AS rats. The intestinal flora count of rats in each subgroup. n = 6. *$p < 0.05$, **$p < 0.01$, ***$p < 0.001$.

the CON subgroup, the level of aortic root fibrosis in the Model subgroup was significantly increased. Compared with the Model subgroup, the level of aortic root fibrosis in the AST IV and Simvastatin subgroups was reduced significantly (Fig. 2A,B). HE staining validated that the intima of the rats in the CON subgroup was smooth, the endothelial cells were arranged regularly, and no atherosclerotic plaque was formed. There were obvious plaques in the aortic wall of the rats in the model subgroup, and the vascular endothelium was damaged and shed. The plaque formation in the aortic wall of rats in the AST IV and Simvastatin subgroups was reduced, and the pathological damage was alleviated (Fig. 2A). qRT-PCR validated tumor necrosis factor-α (*TNF-α*), interleukin-6 (*IL-6*), *IL-1β*, vascular cell adhesion molecule-1 (*VCAM-1*), matrix metalloproteinase-2 (*MMP-2*), macrophage inflammatory protein-1 (*MCP-1*), and intercellular adhesion molecule-1 (*ICAM-1*) mRNA levels were substantially higher in the aortic root tissues of the rats in the Model subgroup compared to the CON subgroup. The *TNF-α*, *IL-6*, *IL-1β*, *VCAM-1*, *MMP-2*, *MCP-1*, and *ICAM-1* mRNA levels were substantially lower in the aortic root tissues of rats in the AST IV and Simvastatin subgroups versus the Model subgroup (Fig. 2C). These results support that AST IV alleviates pathological damage and inflammatory responses in the aortic root and inhibits endothelial dysfunction in AS rats.

AST IV Modulated the Composition of Intestinal Flora in AS Rats

Intestinal flora counts validated substantially lower counts of Bifidobacterium, Lactobacillus, and Bacteroides and substantially higher counts of *Enterobacter*, *Enterococcus*, *Fusobacterium*, and *Clostridium* in the Model subgroup of rats. In contrast with the CON subgroup. The number of Bifidobacterium, Lactobacillus, and Bacteroides in the AST IV and Simvastatin subgroups was substantially augmented, and the number of *Enterobacter*, *Enterococcus*, *Fusobacterium*, and *Clostridium* was significantly reduced versus the Model subgroup (Fig. 3). These results suggest that AST IV can modulate the composition of intestinal flora in AS rats.

AST IV Can Inhibit the PI3K/Akt/mTOR Signaling Pathway in AS Rats

p-PI3K, p-Akt, and p-mTOR protein levels in the aortic root tissue of the Model subgroup were significantly increased compared to the CON subgroup. p-PI3K, p-Akt, and p-mTOR protein levels in the aortic root tissues of AST IV and Simvastatin subgroups were significantly decreased versus the Model subgroup. The western blot confirmed that PI3K, Akt, and mTOR protein levels among the subgroups had no significant difference (Fig. 4). These results reveal AST IV can retain the PI3K/Akt/mTOR signaling pathway in AS rats.

PI3K/Akt/mTOR Signaling Pathway Mediated the Process of AST IV Alleviating AS

BEZ235 (PI3K/Akt/mTOR pathway inhibitor) was employed to intervene in AS rats. Western blot results validated that compared with the AST IV subgroup, p-PI3K, p-Akt, and p-mTOR protein levels in the aortic root tissue of the AST IV + BEZ235 subgroup were significantly decreased (Fig. 5A). In the aortic root tissue of the AST IV + BEZ235 subgroup, qRT-PCR validated that *TNF-α*, *IL-6*,

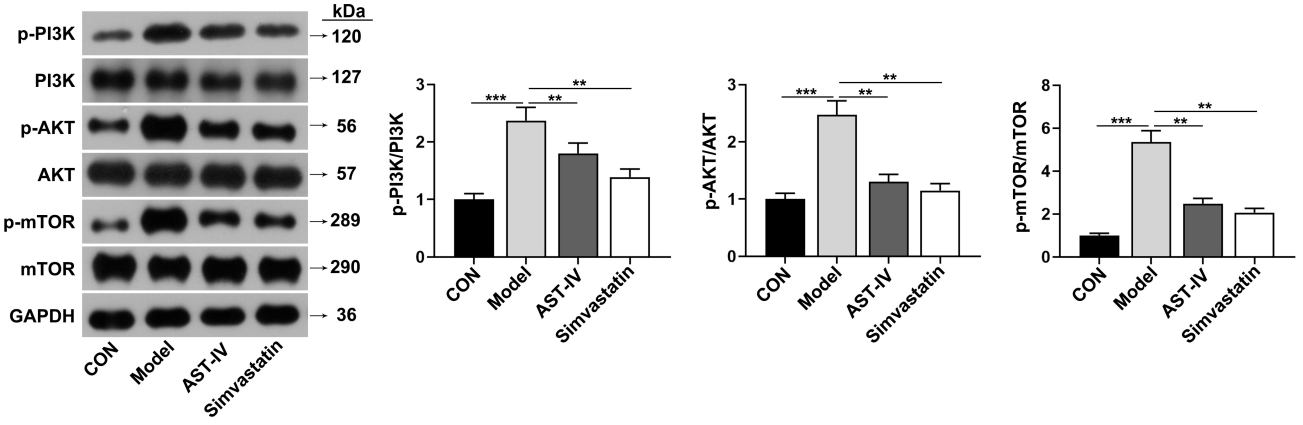

Fig. 4. AST IV can inhibit the PI3K/Akt/mTOR signaling pathway in AS rats. In rat aortic root tissues, p-PI3K, PI3K, p-Akt, Akt, p-mTOR, and mTOR protein levels were appraised via western blot. n = 6. $^{**}p < 0.01$, $^{***}p < 0.001$. p-PI3K, phospho-phosphatidylinositol-3-kinase; PI3K, phosphatidylinositol-3-kinase; p-Akt, p-protein kinase B; Akt, protein kinase B; mTOR, mammalian target of rapamycin; p-mTOR, p-mammalian target of rapamycin.

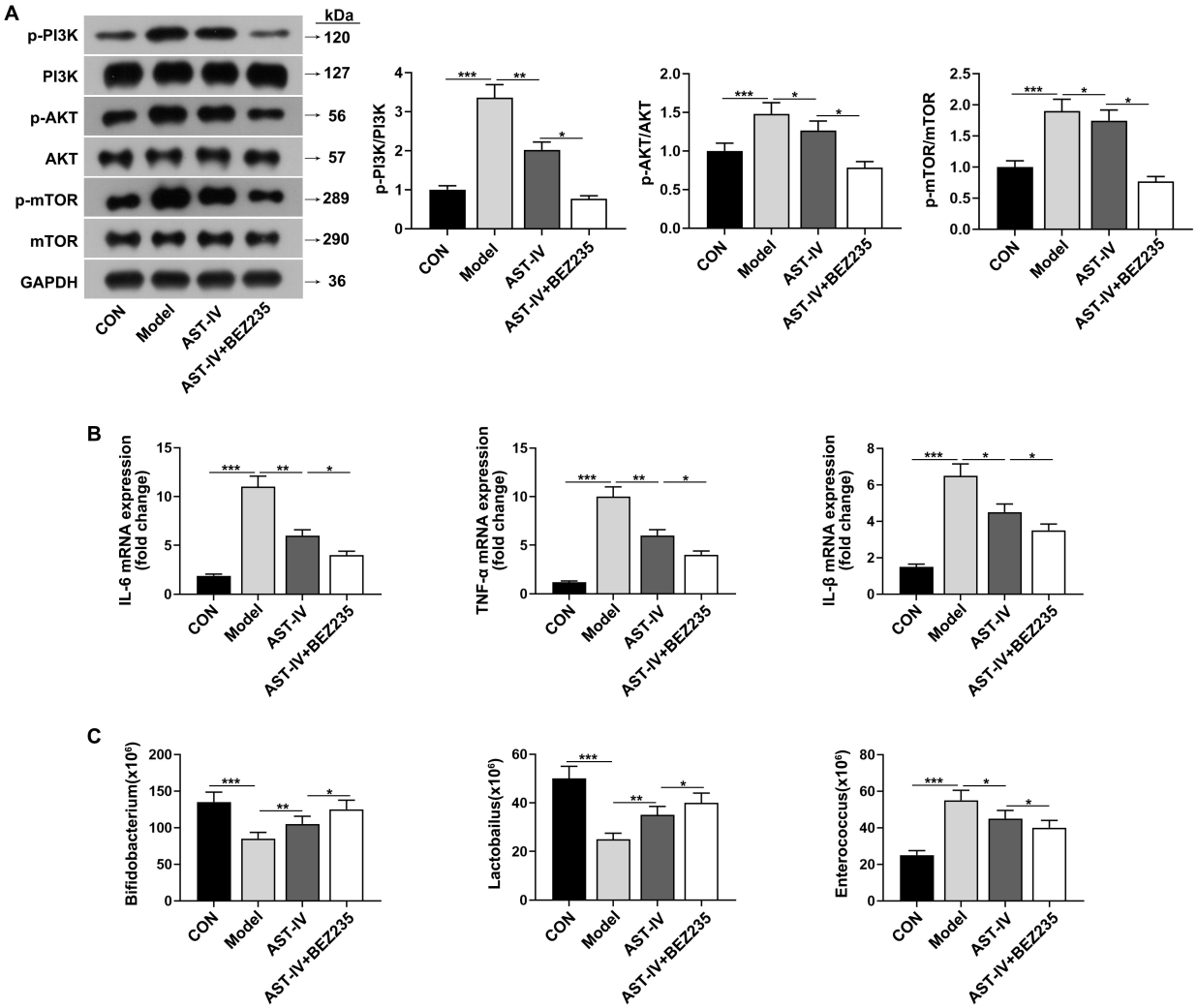

Fig. 5. PI3K/Akt/mTOR signaling pathway mediated the process of AST IV alleviating AS. (A) In rat aortic root tissues, p-PI3K, p-AKT and p-mTOR protein levels were appraised using western blot. (B) *TNF-α*, *IL-6* and *IL-1β* mRNA levels were appraised using qRT-PCR. (C) The counts of *Bifidobacteria*, *Lactobacilli*, and *Enterococcus* in each subgroup of rats. n = 6. $^{*}p < 0.05$, $^{**}p < 0.01$, $^{***}p < 0.001$.

and *IL-1β* mRNA levels were substantially lower than that of the AST IV subgroup (Fig. 5B). Intestinal flora count validated that the number of Bifidobacterium and Lactobacillus in the AST IV + BEZ235 subgroup was substantially augmented, and the number of *Enterococcus* was significantly decreased, compared to the AST IV subgroup (Fig. 5C). These results suggest that the process of AST IV alleviating AS is mediated by the PI3K/Akt/mTOR signaling pathway.

Discussion

AS is a pathological disease characterized by vascular wall fiber proliferation, chronic inflammation, accumulation, and immune disorders [18]. This study employed ApoE$^{-/-}$ rats fed with a high-fat diet as an AS model. The biochemical test results confirmed the blood lipid level of rats in the Model subgroup was substantially augmented, manifested by the increase of serum TC, TG, and LDL-C levels and the decrease of HDL-C levels. The results of the detection of vascular endothelial factors validated that the level of NO in the serum of the Model subgroup eased, and the levels of ET-1 and Ang-II augmented. After administration of AST IV, blood lipid levels and vascular endothelial injury in ApoE$^{-/-}$ rats were substantially increased. The pathological results validated that the aortic lesions in the Model subgroup were evident, the endothelial cells were damaged, and prominent plaque formation was observed in the lumen. After administration of AST IV, the area of the aortic plaque was substantially reduced, and it had an excellent therapeutic effect on AS.

Previous research has shown that chronic inflammation can trigger and promote the development of AS [19]. Proinflammatory cytokines TNF-α, IL-6, and IL-1β are involved in the development of AS, and their blockers have shown promising results in clinical trials [20]. In the initial stage of AS, inflammation damages the vascular endothelium, increases the expression of adhesion molecules (such as VCAM-1 and ICAM-1), and mediates the extravasation of lymphocytes and monocytes from the blood into the subendothelial space [21]. With the progress of AS, the inflammatory response can stimulate the aggregation of macrophages and the expression of MMP (such as MMP-2) in AS plaques, thereby reducing the stability of plaques and leading to plaque rupture [22]. In this study, qRT-PCR validated that *TNF-α*, *IL-6*, *IL-1β*, *VCAM-1*, *MMP-2*, *MCP-1*, and *ICAM-1* levels in the aortic tissue of the Model subgroup were substantially augmented. After administration of AST IV, TNF-α, IL-6, IL-1β, VCAM-1, MMP-2, MCP-1, and ICAM-1 levels in rat aortic root tissue decreased significantly. This indicates that AST IV can alleviate the inflammatory response of AS rats and inhibit endothelial dysfunction in AS rats.

With the deepening of research on intestinal flora, it has been recognized that intestinal flora can play many essential functions in the human body. The intestinal flora is mainly composed of five main phyla: *Firmicutes*, *Bacteroidetes*, *Actinobacteria*, *Proteobacteria*, and *Cerrucomicrobia*. The classification of anaerobic bacteria such as Firmicutes and Bacteroidetes have been shown to contribute more than 90% of healthy gut microbiota composition [23]. A study has shown that *Akkermansia*, *Christensenellaceae*, *Clostridium*, and *Odoribacter* were substantially reduced in the intestinal flora of AS rats. The high abundance of Lactobacillus was related to the increase of HDL. Bifidobacterium has anti-inflammatory effects and has been employed as a probiotic to assist mucosal barrier function and reduce systemic inflammation by controlling the level of lipopolysaccharide in the intestine [24]. Research has previously shown that intestinal flora and its metabolites can play a critical regulatory role in the formation of AS through the reverse transport of cholesterol and the accumulation of cholesterol in macrophages, leading to the formation of atherosclerotic plates by intravascular lipids, cholesterol, calcium, and other substances [8]. In this study, our results validated that AST IV administration substantially augmented the number of intestinal probiotics Bifidobacterium, Lactobacillus, and Bacteroides in rats and eased the number of non-probiotics *Enterobacter*, *Enterococcus*, *Fusobacterium*, and *Clostridium*. This indicates that AST IV can modulate the composition of intestinal flora in AS rats.

PI3K is an intracellular kinase that modulates cell survival, proliferation, migration, differentiation, transcription, and translation in the context of AS by activating signaling pathways. It also plays an important role in the progression and regression of AS, involving endothelial cell apoptosis, lipid accumulation and transport, macrophage autophagy, surface transformation, smooth muscle proliferation, inflammatory response-related adhesion molecule expression, and other physiological processes [25]. Previous study has shown that targeting the PI3K/Akt/mTOR signaling pathway in vascular endothelial cells represents a potential therapeutic target for treating AS [26]. Another study validated that activating the PI3K/Akt/mTOR pathway to modulate LDL-induced autophagy in vascular smooth muscle cells can promote AS [27]. In this study, we found that the protein expression levels of p-PI3K, p-Akt, and p-mTOR in the aorta of the Model subgroup were substantially augmented. After administration of AST IV, the phosphorylation of PI3K, Akt, and mTOR was inhibited significantly. Further studies have found that combining AST IV and the PI3K/Akt/mTOR pathway inhibitor BEZ235 can further inhibit the phosphorylation of PI3K, Akt, and mTOR and alleviate the inflammation level.

Conclusion

To conclude, this study confirmed that AST IV has a potential anti-AS effect. It can improve the pathological changes of the aorta in ApoE$^{-/-}$ rats fed with a high-

fat diet through the PI3K/Akt/mTOR pathway, reduce the level of inflammatory factors, and modulate the composition of intestinal flora. Future investigations will employ 16S rRNA sequencing to delve deeper into the impact of AST IV on the AS-associated gut microbiota at both phylum and genus taxonomic ranks.

Availability of Data and Materials

The datasets analyzed during the current study are available from the corresponding author on reasonable request.

Author Contributions

LHJ has been involved in drafting the manuscript or revising it critically for important intellectual content. LHJ and DWS have made substantial contributions to conception and design, or acquisition of data, or analysis and interpretation of data. YQW and BYP have helped perform the analysis with constructive discussions and supervision and been involved in drafting the manuscript or revising it critically for important intellectual content. All authors contributed to editorial changes in the manuscript. All authors have given final approval of the version to be published. All authors have participated sufficiently in the work to take public responsibility for appropriate portions of the content and agreed to be accountable for all aspects of the work in ensuring that questions related to the accuracy or integrity of any part of the work are appropriately investigated and resolved.

Ethics Approval and Consent to Participate

All experimental protocols of this study were approved by The Affiliated Hospital of Changchun University of Chinese Medicine ethics committee (No: CCZYFYKLL2022-020).

Acknowledgment

Not applicable.

Funding

This research received no external funding.

Conflict of Interest

The authors declare no conflict of interest.

References

[1] Wang X, Yang S, Li Y, Jin X, Lu J, Wu M. Role of emodin in atherosclerosis and other cardiovascular diseases: Pharmacological effects, mechanisms, and potential therapeutic target as a phytochemical. Biomedicine & Pharmacotherapy. 2023; 161: 114539.

[2] Kong P, Cui ZY, Huang XF, Zhang DD, Guo RJ, Han M. Inflammation and atherosclerosis: signaling pathways and therapeutic intervention. Signal Transduction and Targeted Therapy. 2022; 7: 131.

[3] Hooglugt A, Klatt O, Huveneers S. Vascular stiffening and endothelial dysfunction in atherosclerosis. Current Opinion in Lipidology. 2022; 33: 353–363.

[4] Batty M, Bennett MR, Yu E. The Role of Oxidative Stress in Atherosclerosis. Cells. 2022; 11: 3843.

[5] Yang XY, Yu H, Fu J, Guo HH, Han P, Ma SR, *et al*. Hydroxyurea ameliorates atherosclerosis in ApoE$^{-/-}$ mice by potentially modulating Niemann-Pick C1-like 1 protein through the gut microbiota. Theranostics. 2022; 12: 7775–7787.

[6] Huang K, Liu C, Peng M, Su Q, Liu R, Guo Z, *et al*. Glycoursodeoxycholic Acid Ameliorates Atherosclerosis and Alters Gut Microbiota in Apolipoprotein E-Deficient Mice. Journal of the American Heart Association. 2021; 10: e019820.

[7] Sanchez-Rodriguez E, Egea-Zorrilla A, Plaza-Díaz J, Aragón-Vela J, Muñoz-Quezada S, Tercedor-Sánchez L, *et al*. The Gut Microbiota and Its Implication in the Development of Atherosclerosis and Related Cardiovascular Diseases. Nutrients. 2020; 12: 605.

[8] Pieczynska MD, Yang Y, Petrykowski S, Horbanczuk OK, Atanasov AG, Horbanczuk JO. Gut Microbiota and Its Metabolites in Atherosclerosis Development. Molecules. 2020; 25: 594.

[9] Zhou Z, Sun B, Yu D, Zhu C. Gut Microbiota: An Important Player in Type 2 Diabetes Mellitus. Frontiers in Cellular and Infection Microbiology. 2022; 12: 834485.

[10] Schoeler M, Caesar R. Dietary lipids, gut microbiota and lipid metabolism. Reviews in Endocrine & Metabolic Disorders. 2019; 20: 461–472.

[11] Zhang Y, Gu Y, Chen Y, Huang Z, Li M, Jiang W, *et al*. Dingxin Recipe IV attenuates atherosclerosis by regulating lipid metabolism through LXR-α/SREBP1 pathway and modulating the gut microbiota in ApoE$^{-/-}$ mice fed with HFD. Journal of Ethnopharmacology. 2021; 266: 113436.

[12] Abdi M, Esmaeili Gouvarchin Ghaleh H, Ranjbar R. *Lactobacilli* and *Bifidobacterium* as anti-atherosclerotic agents. Iranian Journal of Basic Medical Sciences. 2022; 25: 934–946.

[13] Zhou L, Li M, Chai Z, Zhang J, Cao K, Deng L, *et al*. Anticancer effects and mechanisms of astragaloside IV (Review). Oncology Reports. 2023; 49: 5.

[14] Yang Y, Hong M, Lian WW, Chen Z. Review of the pharmacological effects of astragaloside IV and its autophagic mechanism in association with inflammation. World Journal of Clinical Cases. 2022; 10: 10004–10016.

[15] Sun B, Rui R, Pan H, Zhang L, Wang X. Effect of Combined Use of Astragaloside IV (AsIV) and Atorvastatin (AV) on Expression of PPAR-γ and Inflammation-Associated Cytokines in Atherosclerosis Rats. Medical Science Monitor. 2018; 24: 6229–6236.

[16] Sinaga E, Suprihatin, Yenisbar, Iswahyudi M, Setyowati S, Prasasty VD. Effect of supplementation of Rhodomyrtus tomentosa fruit juice in preventing hypercholesterolemia and atherosclerosis development in rats fed with high fat high cholesterol diet. Biomedicine & Pharmacotherapy. 2021; 142: 111996.

[17] Xu T, Lin T, Xie J, Ren H, Chen N, Wang W. Comparison of antiperitoneal fibrotic effects between an mTORC1-specific blocker and a PI3K/mTOR dual-blocker. Renal Failure. 2019; 41: 267–277.

[18] Xu S, Kamato D, Little PJ, Nakagawa S, Pelisek J, Jin ZG. Targeting epigenetics and non-coding RNAs in atherosclerosis: from mechanisms to therapeutics. Pharmacology & Therapeutics. 2019; 196: 15–43.

[19] Poznyak A, Grechko AV, Poggio P, Myasoedova VA, Alfieri V, Orekhov AN. The Diabetes Mellitus-Atherosclerosis Connec-

tion: The Role of Lipid and Glucose Metabolism and Chronic Inflammation. International Journal of Molecular Sciences. 2020; 21: 1835.

[20] Engelen SE, Robinson AJB, Zurke YX, Monaco C. Therapeutic strategies targeting inflammation and immunity in atherosclerosis: how to proceed? Nature Reviews. Cardiology. 2022; 19: 522–542.

[21] Shi L, Li Y, Xu X, Cheng Y, Meng B, Xu J, *et al*. Brown adipose tissue-derived Nrg4 alleviates endothelial inflammation and atherosclerosis in male mice. Nature Metabolism. 2022; 4: 1573–1590.

[22] Samah N, Ugusman A, Hamid AA, Sulaiman N, Aminuddin A. Role of Matrix Metalloproteinase-2 in the Development of Atherosclerosis among Patients with Coronary Artery Disease. Mediators of Inflammation. 2023; 2023: 9715114.

[23] Tang WHW, Kitai T, Hazen SL. Gut Microbiota in Cardiovascular Health and Disease. Circulation Research. 2017; 120: 1183–1196.

[24] Kurilenko N, Fatkhullina AR, Mazitova A, Koltsova EK. Act Locally, Act Globally-Microbiota, Barriers, and Cytokines in Atherosclerosis. Cells. 2021; 10: 348.

[25] Zhao Y, Qian Y, Sun Z, Shen X, Cai Y, Li L, *et al*. Role of PI3K in the Progression and Regression of Atherosclerosis. Frontiers in Pharmacology. 2021; 12: 632378.

[26] Ji W, Sun J, Hu Z, Sun B. Resveratrol protects against atherosclerosis by downregulating the PI3K/AKT/mTOR signaling pathway in atherosclerosis model mice. Experimental and Therapeutic Medicine. 2022; 23: 414.

[27] Shi G, Zeng L, Shi J, Chen Y. Trimethylamine N-oxide Promotes Atherosclerosis by Regulating Low-Density Lipoprotein-Induced Autophagy in Vascular Smooth Muscle Cells Through PI3K/AKT/mTOR Pathway. International Heart Journal. 2023; 64: 462–469.